Pseudo-Divergence and Bidimensional Histogram of Spectral Differences for Hyperspectral Image Processing

Noël Richard, David Helbert, Christian Olivier, Martin Tamisier

Pseudo-Divergence and Bidimensional Histogram of Spectral Differences for Hyperspectral Image Processing

Noël Richard, David Helbert, Christian Olivier, Martin Tamisier
XLIM Laboratory, UMR 7252 CNRS, University of Poitiers, France.
email: first_Name.Last_Name@univ-poitiers.fr,
tel: +33 5 49 49 66 20

Abstract

Spectral Information Divergence (SID) was identified as the most efficient spectral similarity measure. However, we show that divergence are not adapted to direct use on spectra. Following an idea proposed by Nidamanuri, we construct a spectral pseudo-divergence based on the Kullback-Leibler divergence. This pseudo-divergence is composed of two parts: a shape and an intensity similarity measure. Consequently, bidimensional representation of spectral differences are constructed to display the histograms of similarity between a spectral reference and the spectra from a data-set or an hyperspectral image. We prove the efficiency of the spectral similarity measure and of the bidimensional histogram of spectral differences on artificial and Cultural Heritage spectral images.

Index Terms

Hyperspectral, spectral distance, spectral similarity, Kullback-Leibler divergence, spectral discrimination.

I. Introduction

The recent advances in imaging allow to acquire images with several hundred of channels in the visible and/or the invisible range of wavelengths. Such spectral accuracy takes a big interest in control by vision or in cultural heritage applications [1], [2], [3]. After several years of developments in spectral imaging, a new level of processing is required to reach a metrological level taking benefits of this important spectral resolution. Under this sense, we express the requirement to develop generic, reproducible and accurate processing [4].

In hyperspectral imaging, reflectance and radiance spectra are analyzed. In the two cases, the initial spectral properties are continuous and sampled with a high resolution and without overlapping. Due to the multi-channel acquisition, spectra are generally consider as vectors [5], [6] with dedicated distances measures based on L_2(Euclidean) constructions or angular difference estimations. Such definitions are not unique, other searchers considering spectra as distributions in an equivalent form to probability density functions[7], [8], [9]. In these cases, several forms of divergence and similarity measures are considered from the basic Kullback-Leibler to more complex ones. More recently, some authors proposed to consider spectra as lattices or manifold [10], [11], [12], using essentially ISOMAP structures for distances assessments. Even if spectra was never associated to the definition of sequences, the associated distances was compared to the others approaches in [13], [14].

In [15] the authors expressed the limits of the distance/similarity measures in front of the visual inspection, which can judge two spectra as spectroscopically dissimilar, even if they was mathematically nearly identical. Several works were dedicated to the selection of the better spectral distance/similarity measures using existing databases[16], [17], [18]. In [13], [14], we develop the theoretical relationship existing between these distance/similarity measures and the spectrum definition. Then using artificial spectra, limits in the existing distance/similarity measures were shown. Finally, similarity measures, considering the spectrum as a probability density function, was identified as the most efficient in front the other measures.

The most interesting proposition was proposed in [15] by defining the Normalized Spectral Similarity Score (NS^3). This score combines two measures, one assessing the shape similarity based on a Spectral Angle Measure (SAM) and a second one based on the L_2 (Euclidean) difference of the two considered spectra. In this work, we propose to kept this idea in order to construct Bidimensional Histograms of Spectral Differences (BHSD) using an adapted distance/similarity measures.

In a first step, we will come back on the nature of spectra in hyperspectral imaging, and especially on the continuous nature of the initial spectrum (sec. II-A). Then we recall some main used expressions to assess the distance/similarity measure between two spectra (sec. II-B and II-C). We show then how to develop an adapted spectral similarity measure using the Kullback-Leibler divergence. Especially, we will show how this construction naturally embed a shape similarity measure, and a measure about the energy difference between the spectra. Limits of the used spectral distance/similarity measures will be compared in the section IV using artificial data-sets. Then the application of these similarity measures and bidimensional histogram of spectral differences will be developed in an application from cultural-heritage domain (sec. IV-D).

II. Spectral distances and divergences

In spectral imaging, two kinds of spectra are considered, radiance and reflectance spectra. The first one corresponds to the energy spectrum emitted by a source and acquired by a spectral sensor. In this case, the surface is considered as a source emitting a continuous radiance. Consequently, the unit is expressed in Watt(W) per square meter(m^2) for each wavelength channel expressed in nanometers (nm). So the unit of radiance spectra is expressed in $W.m^{-2}.nm^{-1}$. The second one corresponds to the reflectance spectrum allowing to assess the ability of a surface to reflect the light in the direction of the sensor. So, the obtained measure is a percentage of the transmitted energy over the wavelength. In the two cases, spectra are expressed on their spectral domain of acquisition between $\lambda_{\min}$ and $\lambda_{\max}$:

$$S = \{s(\lambda), \forall \lambda \subset [\lambda_{\min}, \lambda_{\max}]\} \tag{1}$$

A. Sum or integral for distance/similarity expressions?

The initial consideration for spectral distance/similarity measure assessment is then to consider it in the continuous domain of expression. For example, by considering the spectra as a vector and by using a L_2 metrics (or p-order Minkowski distance), the distance measures will be expressed as:

$$d_{L_2}(S_1, S_2) = \left(\int_{\lambda_{\min}}^{\lambda_{\max}} (s_1(\lambda) - s_2(\lambda)|^p \right)^{\frac{1}{2}} d\lambda \tag{2}$$

Due to the spectral sampling at the core of the spectroradiometer or spectral sensors, discrete versions of the distance functions are used, like in the equation 3. Nevertheless, in such expressions the relationship to the initial continuous signal is always forgotten. Such lack induces two main limits, firstly the link to the distance unit is loosed and secondly the distance measures between spectra can not be independent from the spectral resolution of sensors.

$$d^d_{L_2}(S_1, S_2) = \left(\sum_{k_\lambda=0}^{k_{\max}} (s_1(k) - s_2(k))^2 \right)^{\frac{1}{2}} \tag{3}$$

with k corresponding to the channel index associated to the wavelength range: $[\lambda_{\min} + k \cdot \Delta_\lambda ; \lambda_{\min} + (k+1) \cdot \Delta_\lambda [$.

In order to progress in a short future toward a spectral metrology, we selected to preserve the continuous integration, and so to preserve the link to the physical content. We assume the fact that the reader can easily adapt these expressions in an equivalent discrete version taking attention to the considered wavelength range and to the wavelength sampling. Now, we will express some main used distance and similarity measures, starting by measures considering the spectrum as a vector, then by measures considering it as a probability density function.

B. Distance measures for spectra considered as a vector

Since the last fifteen years, a large number of distances and similarity measures was tried and used to analysis spectral data. The most popular own to the group of measures considering the spectrum as a vector in an n-dimensional vector space. Such choice implies that the vector is represented as n-tuples where each channel measure is considered as independent to the others. The most used distance measures in the spectral domain are deduced from the L_p metrics as for example in [19], [20], [21]:

$$d_{L_p}(S_1, S_2) = \left(\int_{\lambda_{\min}}^{\lambda_{\max}} |s_1(\lambda) - s_2(\lambda)|^p \, d\lambda \right)^{\frac{1}{p}}, \tag{4}$$

$$d_{\chi^2_1}(S_1, S_2) = \int_{\lambda_{\min}}^{\lambda_{\max}} \frac{(s_1(\lambda) - s_2(\lambda))^2}{s_1(\lambda) + s_2(\lambda)} d\lambda \tag{5}$$

$$d_{Can}(S_1, S_2) = \int_{\lambda_{\min}}^{\lambda_{\max}} \frac{|s_1(\lambda) - s_2(\lambda)|}{s_1(\lambda) + s_2(\lambda)} d\lambda \tag{6}$$

where d_{L_p} is the L_p distance, $d_{\chi^2_1}$ one of the two χ^2 similarity measure and d_{Can} the Canberra measure.

Even if these distance functions are often used, they are limited in their assessment of shape dissimilarity[14]. Typically, if we consider two non-overlapped spectra, first one defined on $[\lambda_0, \lambda_1]$ and the second one on $[\lambda_2, \lambda_3]$, with $\lambda_2 > \lambda_1$, whatever is the slicing $(\lambda_1 - \lambda_2)$, the spectral distance is always dependant to the cumulative energy of each spectrum:

$$\int_{\lambda_{\min}}^{\lambda_{\max}} |s_1(\lambda) - s_2(\lambda)|^p d\lambda = \int_{\lambda^1_{\min}}^{\lambda^1_{\max}} |s_1(\lambda)|^p d\lambda + \int_{\lambda^2_{\min}}^{\lambda^2_{\max}} |s_2(\lambda)|^p d\lambda$$

with

$$\lambda_{\min} < \lambda^1_{\min} < \lambda^1_{\max} < \lambda^2_{\min} < \lambda^2_{\max} < \lambda_{\max} : \begin{cases} s_1(\lambda) = 0 & \forall \lambda \in [\lambda_{\min}, \lambda^1_{\min}[\cup]\lambda^1_{\max}, \lambda_{\max}[\\ s_2(\lambda) = 0 & \forall \lambda \in [\lambda_{\min}, \lambda^2_{\min}[\cup]\lambda^2_{\max}, \lambda_{\max}[\end{cases} \tag{7}$$

As radiance or reflectance spectra rarely include null values in the relectance/radiance series, such limitations are difficult to perceive in real cases. But if we consider a spectrum as a sum of basic functions linked to the physical properties of surfaces and light, these limitations are problematic.

Another way to assess the similarity between two vectors is to limited it to a shape difference. The most direct expression on this way estimates the angle between two n-dimensional vectors through the dot product [22]. In spectral imaging, the obtained angle is known as the Spectral Angle Mapper (eq. 8) and is defined between 0 and $\frac{\pi}{2}$ [23]. A normalization relative to the total amount of energy of the two spectra is applied inside the angle calculation to obtain the independency to the illumination changes.

Another form is sometimes preferred using the cosinus of the spectral angle to obtained value between 0 and 1, with smallest values for closest spectra (eq. 8).

$$P = \frac{\int s_1(\lambda)s_2(\lambda)d\lambda}{\sqrt{\int s_1(\lambda)^2 d\lambda}\sqrt{\int s_2(\lambda)^2 d\lambda}}, \qquad \begin{array}{ll} d_{\mathrm{SAM}}(S_1,S_2) & = \arccos(P) \\ d_{\cos}(S_1,S_2) & = 1-P \end{array} \tag{8}$$

Nevertheless, when the intersections of spectra becomes null, the distance is also saturated as in the previous cases. Such behaviour is fully understandable. Due the nature of the spectra they can not be considered as vectors, because the acquired hyperspectral channels produce an ordered sequence of measures, physically correlated.

C. Distance measures for Spectra considered as a distribution

In [16], [18], [17], authors compare the discrimination performances of distance/similarity measures on different spectrum databases or spectral image databases. They conclude that *Spectral Information Divergence* is the most efficient spectral similarity measure. Such similarity measure assumes that a spectrum can be considered as a probability density function, so a distribution. Such hypothesis is correct in accordance to the formation of spectrum defined by a sequence of energy measures over the wavelengths. So this hypothesis directly assumes the high correlation between neighbored spectral bands [24]. From this hypothesis, authors proposed to work with different kinds of divergence or cumulative distribution functions [25], [8], [9]. If we expect the basic forms of divergence similar to the Euclidean distances, the proposed divergence measures are :

$$d_{\mathrm{Smi}}(S_1,S_2) = 1 - \frac{\int_{\lambda_{\min}}^{\lambda_{\max}} \min(s_{1,\lambda}, s_{2,\lambda})d\lambda}{\min(\int_{\lambda_{\min}}^{\lambda_{\max}} s_{1,\lambda}d\lambda, \int s_{2,\lambda}d\lambda)} \tag{9}$$

$$d_{\mathrm{Jef}}(S_1,S_2) = \int_{\lambda_{\min}}^{\lambda_{\max}} s_1(\lambda)\log\frac{2.s_1(\lambda)}{s_1(\lambda)+s_2(\lambda)}d\lambda + \int_{\lambda_{\min}}^{\lambda_{\max}} s_2(\lambda)\log\frac{2.s_2(\lambda)}{s_1(\lambda)+s_2(\lambda)}d\lambda \tag{10}$$

$$d_{\mathrm{Pea}}(S_1,S_2) = \int_{\lambda_{\min}}^{\lambda_{\max}} \frac{\left(s_1(\lambda)-m(\lambda)\right)^2}{m(\lambda)}d\lambda \qquad \text{with } m(\lambda) = \frac{s_1(\lambda)+s_2(\lambda)}{2} \tag{11}$$

where d_{Smi}, d_{Jef} and d_{Pea} are respectively the Smith, Jeffrey and Pearson divergence measures. Inside this family of similarity measure the most used in the spectral literature is the Spectral Information Divergence (SID), also known as the Kullback-Leibler divergence. This particular measure will be developed in the section III.

Due to their construction, these functions present less or more the same limitations than the distance/similarity measures derived from the L_2(Euclidean) form. Obviously, the L_2(Euclidean) distance based on the cumulated spectra (ECS) solves this limit in the shape difference analysis [14]. In fact this similarity measure is based on the similarity of Cumulative Distribution Function.

$$d_{\mathrm{ECS}}(S_1,S_2) = \sqrt{\int_{\lambda_{\min}}^{\lambda_{\max}} \left(\widehat{s_1}(\lambda)-\widehat{s_2}(\lambda)\right)^2 d\lambda}, \qquad \text{with } \widehat{s_i}(\lambda_c) = \int_{\lambda_{\min}}^{\lambda_c} s_i(\lambda)d\lambda. \tag{12}$$

The ECS similarity measure embeds as in a whole the spectral shape and intensity similarities. When only shape differences are expected for the spectral discrimination, specific measures can be developed. In [26], the authors expressed the proximity between the Pearsonian Correlation Coefficient and the Spectral Angle Mapper. Thanks to this proximity they proposed to use the Pearsonian correlation coefficient to express an angle measurement between spectra considered as distributions. This similarity measure is known as the Spectral Correlation Mapper (eq. 13)[27] and must be compared to the $d_{\cos}$ measure (eq.8). The associated angle d_{SCM_α} is then directly obtained using an inverse cosinus transform (eq.14)[27]. To note that another interesting form, close in the writing form, was proposed in [28] as the Cross Correlogram Spectral Matching (CCSM) and named after Spectral Correlation Measure(SCM) in [18].

$$d_{\text{PearCor}}(S_1,S_2) = \frac{\int (s_1(\lambda)-\mu_{S_1})(s_2(\lambda)-\mu_{S_2})d\lambda}{\sqrt{\int (s_1(\lambda)-\mu_{S_1})^2 d\lambda}\sqrt{\int (s_2(\lambda)-\mu_{S_2})^2 d\lambda}} \quad \text{with} \begin{cases} \mu_{S_1} = \frac{\int s_1(\lambda)d\lambda}{\lambda_{\max}-\lambda_{\min}} \\ \mu_{S_2} = \frac{\int s_2(\lambda)d\lambda}{\lambda_{\max}-\lambda_{\min}} \end{cases}$$

$$d_{\text{SCM}}(S_1,S_2) = 1 - \frac{1+d_{\text{Pea}}(S_1,S_2)}{2} \tag{13}$$

$$d_{\text{SCM}_\alpha} = \arccos(d_{\text{Pea}}(S_1,S_2)) \tag{14}$$

D. The searched distance between spectra

In [15], authors expressed that Spectral Angle Measure (SAM) "*can readily discriminate quite dissimilar materials such as vegetation from non-vegetation features ...*". Nevertheless, farthest in this work they expressed the limits in the angle assessment for spectral discrimination, when dissimilarities are more linked to intensity variations. In this second case, using L_2(Euclidean) forms of distances/divergence measures are more adapted, but in this case, the shape variations can be under-evaluated. To solve this constraint, authors constructed a score (Normalized Spectral Similarity Score: NS^3). This score combines an angle measurement based on the d_{cos} similarity measure and a measure from the L_2 distance for the energetic difference. This energetic difference is the root mean square difference between the two spectra averaged over the spectral range of observation (d_{RMS}) as proposed by [23]. Then the Normalized Spectral Similarity Score is defined by the following quadratic form:

$$d_{\text{NS}^3}(S_1,S_2) = \sqrt{(d_{\text{RMS}}(S_1,S_2))^2 + (d_{\cos}(S_1,S_2))^2}. \tag{15}$$

The proposed construction embeds as a whole a shape and an intensity difference in a global measure. Such construction is to compare to perceptual colour distance in colorimetry [29], where the hue difference can be a part of the perceptual distance ΔE. Nevertheless, the NS^3 score is empirically constructed. The quadratic form used in the construction is selected by the authors to define an Euclidean form. But such construction is valid if the two measures (d_{RMS} and $d_{\cos}$) are independent. As d_{RMS} is sensible to shape changes, such hypothesis is not enabled.

If the ideal spectral distance/similarity don't yet exist, we have defined the constraints to solve in order to define it. This searched measure must be correlated to spectral modifications between a spectral reference and a modified spectrum from this reference [14]. In addition, it must be composed at least of two parts describing the shape difference and the intensity difference [15], in order to help in the discrimination process. In the following section we develop one expression respecting these constraints.

III. An adapted spectral similarity measure

Since Jeffrey [30], divergence measures are designed to measure the dissimilarity between probability functions. In 1951, S. Kullback and R.A. Leibler defined in [31] the "*mean information for discrimination between two probability distributions*" as:

$$\text{KL}(H_1,H_2) = E_{H_1}\left[\log\left(\frac{H_1}{H_2}\right)\right] = \int_{-\infty}^{\infty} h_1(x)\log\left(\frac{h_1(x)}{h_2(x)}\right)dx, \tag{16}$$

where $E_{H_1}[.]$ denotes the expectation value with respect to the probability density H_1.

The $KL(H_1,H_2)$[1] measure expresses the quantity of information loose when H_2 is used to estimate H_1. Then Kullback and Leibler expressed the *divergence* between the probability laws in a symmetric and nonnegative measure as:

$$\text{div}_{\text{KL}}(H_1,H_2) = \int_{-\infty}^{\infty}(h_1(x)-h_2(x))\log\left(\frac{h_1(x)}{h_2(x)}\right)dx \triangleq \text{KL}(H_1,H_2)+\text{KL}(H_2,H_1). \tag{17}$$

Using KL divergence in spectral imaging is classic and known as the Spectral Information Divergence (SID)[32], [7].

A. Normalized spectra

Divergence measures was designed to measure the similarity between probability density functions. So to obtain valid similarity measures, the signals to analyze must respect the construction constraints of probability density functions : to be a set of measures ordered in accordance to an acquisition criteria, and to have an integral over the full range of the criteria equal to one. This second constraints corresponds to the equation 18 in the spectral case. Respecting this constraint allows to obtain similarity measures assessing only to the shape dissimilarities between the two signals.

$$\int_{\lambda_{min}}^{\lambda_{max}} h_i(x)dx = 1. \tag{18}$$

[1]denoted as $I(1:2)$ in the original article.

In order to applied KL-divergence on valid signals, we define the normalized spectrum $\overline{S}$ from the initial spectrum S. Be a reflectance spectrum S or energy spectrum defined on $[\lambda_{min}, \lambda_{max}]$, the normalized spectrum is defined by:

$$\overline{S} \quad = \quad \left\{ \overline{s}(\lambda) = \frac{s(\lambda)}{k}, \forall \lambda \subset [\lambda_{\min}, \lambda_{\max}] \right\} \text{and } k = \int_{\lambda_{min}}^{\lambda_{max}} s(\lambda) d\lambda. \tag{19}$$

B. The spectral Kullback-Leibler pseudo-divergence

In order to develop a similarity distance solving the constraints expressed in section II-D, we select to start using the Kullback-Leibler(KL) divergence. In the following section, we will link the KL divergence measure applied on normalized spectra to a measure applied on the initial spectra, defined as a pseudo-divergence[2]. We will show that thanks to this construction we obtain the expected similarity measure including two parts : one dedicated to shape discrimination and another one dedicated to the global intensity difference.

1) The spectral pseudo KL information for discrimination: Starting from the Kullback-Leibler measure of information for discrimination (eq. 16) applied on normalized spectra $\overline{S}$, we replace them using the normalization weights k and the full spectra S:

$$\mathrm{KL}(\overline{S}_1, \overline{S}_2) \quad = \quad \int_{\lambda_{min}}^{\lambda_{max}} \overline{s}_1(\lambda) \log \left(\frac{\overline{s}_1(\lambda)}{\overline{s}_2(\lambda)} \right) d\lambda = \frac{1}{k_1} \int_{\lambda_{min}}^{\lambda_{max}} s_1(\lambda) \log \left(\frac{s_1(\lambda)}{s_2(\lambda)} \right) d\lambda + \log \left(\frac{k_2}{k_1} \right) \int_{\lambda_{min}}^{\lambda_{max}} \frac{s_1(\lambda)}{k_1} d\lambda. \tag{20}$$

As $\int_{\lambda_{min}}^{\lambda_{max}} \frac{s_1(\lambda)}{k_1} d\lambda = 1$, we arrive to a basic and nice relationship introducing the spectral pseudo-information of discrimination between the full spectra S_1 and S_2 (eq. 21). So the spectral pseudo-information of Kullback-Leibler $\mathrm{KL}'(S_1, S_2)$ can link to the spectral information of Kullback-Leibler $\mathrm{KL}(\overline{S}_1, \overline{S}_2)$ applied on normalized spectra $\overline{S}_1$ and $\overline{S}_2$ (eq. 22):

$$\mathrm{KL}(\overline{S}_1, \overline{S}_2) \quad = \quad \frac{1}{k_1} \int_{\lambda_{min}}^{\lambda_{max}} s_1(\lambda) \log \left(\frac{s_1(\lambda)}{s_2(\lambda)} \right) d\lambda + \log \left(\frac{k_2}{k_1} \right) \tag{21}$$

$$\mathrm{KL}'(S_1, S_2) \quad = \quad k_1 \left(\mathrm{KL}(\overline{S}_1, \overline{S}_2) \right) - k_1 \log \left(\frac{k_2}{k_1} \right). \tag{22}$$

It is interesting to note that the spectral KL-pseudo-information (eq. 22) is composed of two parts. The first one is correlated to the shape variations between the two spectra, due to the KL-divergence on the normalized spectra. The second one is correlated to the spectral difference according to the total energy/reflectance.

2) The spectral KL pseudo-divergence: Following the construction proposed by Kullback and Leibler in order to obtain a symmetrical measure from the information measure (eq. 17), it is easy to demonstrate that the relationship between information and divergence is also valid between pseudo-information and pseudo-divergence:

$$div_{\mathrm{KL}'}(S_1, S_2) = KL'(S_1, S_2) + KL'(S_2, S_1). \tag{23}$$

Replacing in the previous equation the pseudo-informations by their expressions from equation 22, we obtain then the final expression for the spectral KL-pseudo-divergence:

$$div_{\mathrm{KL}'}(S_1, S_2) \quad = \quad k_1 KL(\overline{S}_1, \overline{S}_2) + k_2 KL(\overline{S}_2, \overline{S}_1) + (k_1 - k_2) \log \left(\frac{k_1}{k_2} \right). \tag{24}$$

Thanks to the expression 24 we have a similarity measure, called pseudo-divergence, due to the fact that radiance/reflectance spectra can not be considered as probability function. This similarity measure is composed of two parts, the first one assessing shape similarities and the second one intensity variations. In the following section we will assess the interest of such similarity measure.

IV. Results and applications

We develop the assessment of this new spectral similarity measure under three points of view. First one will explore the validation criteria defined in [14] using artificial spectra constructed using Gaussian functions. This first validation level will enable that the expected theoretical properties are respected. The second point of view will allow to analyze the discrimination between shape and intensity using bidimensional histogram of spectral differences. Finally, we will explore how this new similarity measure associated to this bidimensional histogram of spectral differences can be interesting for Cultural Heritage applications.

[2]The divergence term can be only used for data respecting the constraints of probability density functions, as we kept the form of the divergence expression the term pseud-divergence is more adapted.

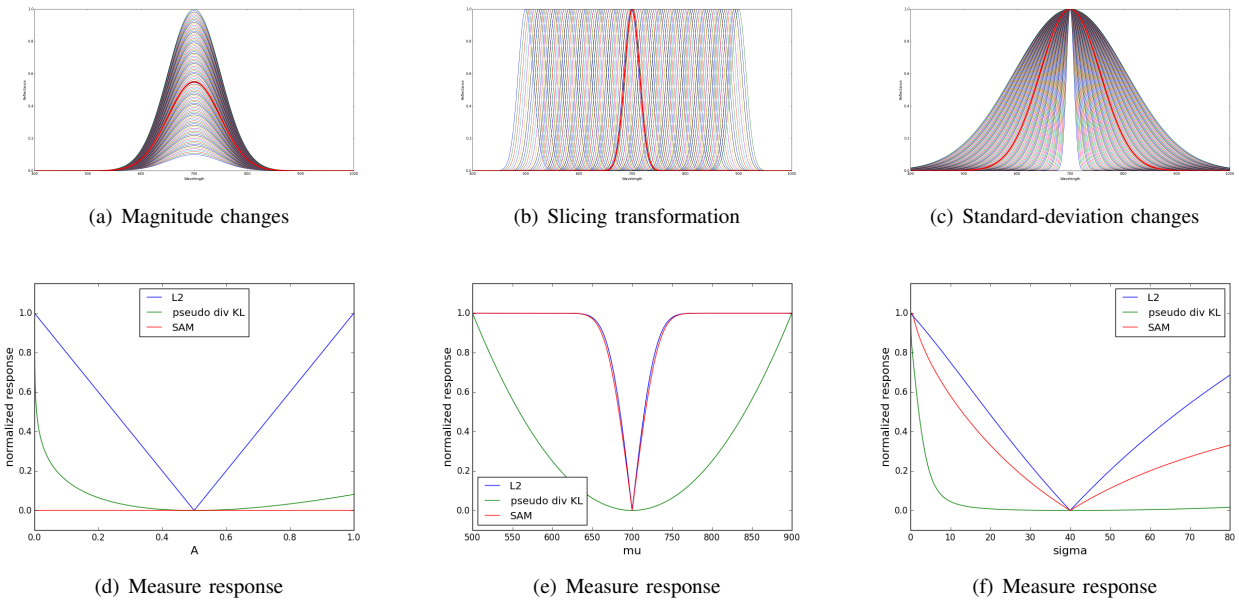

(a) Magnitude changes (b) Slicing transformation (c) Standard-deviation changes

(d) Measure response (e) Measure response (f) Measure response

Fig. 1. Basic transformations and associated responses of spectral L_2 distance, SAM similarity and KL-pseudo-divergence measures.

A. *Pseudo-divergence response to basic spectral transformations*

In order to compare the spectral distance and similarity measure, a behaviour constraint is proposed in [13] then in [14]. The constraint implies that a valid distance/similarity measure must be correlated to the transformation parameter, used to transform an initial spectrum, whatever the parameter value is. To assess the validity of an important set of distance/similarity measures, we selected to use a Gaussian function[3] and three kinds of transformation: magnitude change, translation over the wavelengths and standard-deviation changes, which was not assessed in the previous works.

Figure 1 shows the 3 data-sets, in first case (fig 1.(a)) the transformation modifies the Gaussian magnitude without modifying the standard-deviation (no energy preservation). The parameter range varies from values lower than the unity to two units. The spectral reference is drawn in red and corresponds to a parameter equal to one. For the second data-set (fig 1.(b)), the applied transformation is a translation over the wavelengths. The used parameter range allows to explore spectrum locations around the reference (red curve) with a displacement corresponding to at maximum twice the larger of the reference spectrum. In the third data-set (fig 1.(c)), we explore the impact of shape modifications varying the standard-deviation. The reference spectrum is always drawn in red at the middle of the parameter range.

In this work, we compare the KL-pseudo-divergence(*KLPD*) to SAM similarity and to the L_2 (Euclidean) distance measures as the most used measures. The proposed results will be directly comparable to an extended set of distance/similarity measures in [14]. So in this work the purpose is only to assess the performance of the KL-pseudo-divergence with the two most known approaches.

Without surprise, the L_2 and *KLPD* measures are able to assess a magnitude variation between spectra and SAM is not sensible to change in intensity (fig 1.(d)). Even if the dynamic of the *KPLD* is not symmetric due to the logarithmic expression, the similarity is not saturated. As developed previously, L_2 (Euclidean) and SAM measures saturate when the intersection between spectra becomes null (fig 1.(d)). In this case, the shape similarity measure at the core of the *KLPD* ensures the response symmetry. In the third case, as the intersection between spectra is preserved, the three distance measures can be correlated to the parameter variations (fig 1.(d)). Even if the *KLPD* seems saturated, it is not the case (see Appendix). In [14], we conclude that ECS similarity measure respects the constraints of response to basic transforms. However, the ECS similarity measure do not naturally separate shape variations from intensity variations. Consequently, it can not be retain for the following parts of this work.

B. *Bidimensional Histograms of Spectral Differences (BHSD)*

Thanks to the idea to decompose a spectral distance/similarity measure in two parts, we propose to create bidimensional representations of spectral differences. Such construction becomes crucial to assess or characterize distributions of spectra. The mean interest of Bidimensional Histogram of Spectral Differences (BHSD) is to be easy to understand.

[3]As the purpose is to assess the correlation between the measure and the transformation parameter, there is no interest to use a more complex spectrum.

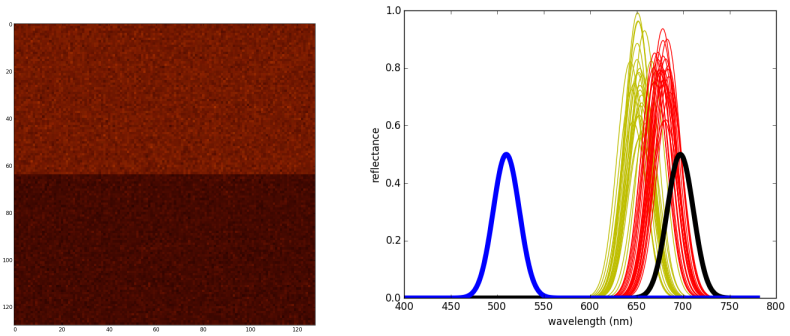

(a) Bicolour synthetic image.

(b) Spectra from the two subsets (yellow and red curves) and chosen references (black and blue curves).

Fig. 2. Image generated using randomly transformed Gaussian functions.

In the following, we proposed to compare three kinds of bidimensional representation. The first one comes directly from the Nidamanuri and Zbell proposition [15], using as horizontal axis the $d_{\cos}(S_1,S_2)$ measure coming from the SAM measures; and as vertical axis the L_2(Euclidean) distance between the two spectra $d_2(S_1,S_2)$ (eq.25). As explained in section II-D, the proposed construction by Nidamanuri is not optimal. So, for the second construction, we propose a direct construction using the angle measure using $d_{\mathrm{SAM}}(S_1,S_2)$ for the horizontal axis and the difference of the cumulated energy for the vertical axis (eq.26). Finally, the third representation is directly deduced from the spectral KL-pseudo-divergence (*KLPD*) using $\left(k_1 KL(\overline{S}_1,\overline{S}_2) + k_2 KL(\overline{S}_1,\overline{S}_2)\right)$ (shape similarity) as horizontal axis and $(k_1-k_2)\log\left(\frac{k_1}{k_2}\right)$ (energy similarity) as vertical axis (eq.27).

$$BHSD_{NS^3} \quad : \quad \begin{cases} \text{shape} & : 1 - d_{\cos}(S_1,S_2) \\ \text{energy} & : L_2(S_1,S_2) \end{cases} \tag{25}$$

$$BHSD_{SAM} \quad : \quad \begin{cases} \text{shape} & : SAM(S_1,S_2) \\ \text{energy} & : \int_{\lambda_{min}}^{\lambda_{max}} (s_1(\lambda) - s_2(\lambda))\, d\lambda \end{cases} \tag{26}$$

$$BHSD_{KLPD} \quad : \quad \begin{cases} \text{shape} & : k_1 KL(\overline{S}_1,\overline{S}_2) + k_2 KL(\overline{S}_2,\overline{S}_1) \\ \text{energy} & : (k_1-k_2)\log\left(\frac{k_1}{k_2}\right) \end{cases} \tag{27}$$

The comparison will be developed in two cases. Firstly, we illustrate the discrimination ability offered by a BHSD structure in the case of an artificial spectrum set, then on data coming from Cultural Heritage.

C. BHSD applied on artificial dataset

For this first experiment we consider an image composed of two non-uniform regions, defined by a particular distribution of spectra (fig. 2.(a)). These distributions are defined by basic transformations (magnitude, spectral slicing, standard-deviation) applied on a Gaussian function. The two initial Gaussian functions are close with non-null intersection. The transformation parameters are randomly selected using a uniform distribution. Some spectra coming from the two subsets are visible in figure 2.(b) in yellow and red. The black and blue spectra are two references used to process the BHSD. The distance/similarity measures are computed between the spectrum at each location and the reference. The first reference (black) is chosen as being closest to the shape of the two spectral distributions, rather than the second reference as farthest (null intersection).

Figure 3 presents the three Bidimensional Histograms of Spectral Differences, where the distances/similarities are computed between the spectra from image in figure 2.(a) and the reference drawn in black (fig. 3.(b)). In the three cases, the two distributions are clearly discriminated. For the representation coming from the NS^3 score (fig. 3.(a)), as the shape measure is correlate to the intensity measure, the distribution hull is organized among the diagonal. The non-linearity in the SAM response, and consequently in the cosinus extracted from the spectral angle explains why the two distributions have not the same size on the horizontal axis. For the second BHSD representation using the SAM and the difference of cumulated energy (fig.3.b), the non-linearity in the angle assessment of SAM explains the shape difference between the histograms of two subsets. The difference of the total energy as vertical axis allows to remove the correlation between axis, solving the problem presented in NS^3 score.

Figure 3.(c) finally presents the Bidimensional Histogram of Spectral Differences processed using the two parts of the spectral KL-pseudo-divergence. The first distribution starting from the left is the closest one from the reference, corresponding to the red spectra in figure 2.(b). Non-linearity of the KLPD shape similarity measure also induces differences in the horizontal size of the spectral difference distributions.

As no constraint can be imposed on reference location and shape, in a second experiment we consider a reference far from the initial spectral sets (blue reference in figure 2.(b). Figure 4 shows the corresponding BHSD. As explained in section II-B, due to the null intersection between the reference and the spectra from the two distributions, the SAM measure and the associated cosinus version (NS^3 case) are saturated. Consequently the angle measurement can not express the shape variations (fig. 4.(a) and 4.(b)). Rather than the proposed representation based on the spectral KL-pseudo-divergence (fig. 4.(c)) that allows to well represent the two spectral distributions. To note slicing the reference over wavelengths changes the range of shape variations from $[0;450]$ to $[1500;4500]$ (fig. 3.(c) and 4.(c)).

D. Applications of BHSD on Cultural Heritage applications

In Cultural Heritage domain, it is crucial to identify pigments in painting without destructive approaches. In this context, hyperspectral imaging offers a real solution only limited by the lack of accuracy in spectral distance assessment. Thanks to the spectral KL-Pseudo-Divergence (KLPD) and to the Bidimensional Histogram of Spectral Differences (BHSD), we propose a solution to this limit.

For this applicative part, we show the interest of the proposed solutions to analyze the spectral distribution of some colours from the *Borbonicus codex*[4]. The hyperspectral images from the *Borbonicus codex* was acquired by the Research Center on the Collection from the French National Museum of Natural History. Page 30 is presented in figure 5.(a) using Colour Matching Functions (CMF) to transform the spectral image into *RGB* colour space [34]. This image was acquired using an hyperspectral sensor in the visible range (840 channels between 400*nm* to 1000*nm*, 1600×1700 pixels/page).

1) BHSD to analyze spectral distribution of colour: In a first experiment, we will take attention to the green colour of this page 30. The spectra corresponding to the green colour is selected using a threshold and validated by experts. In figure 5, we show some of the selected spectra and their corresponding colour.

In a first consideration, we select the spectrum drawn in red in figure 5.(b) as the reference to analyze the spectral distribution of green pigments. The Bidimensional Histogram of Spectral Differences of the green pixels is presented in figure 6.(c). In this figure, we added also the unidimensional histograms corresponding to the shape (chromatic) and intensity similarities. As the similarity measures are positive and as the reference is in the middle of the spectral distribution, the spectral distribution presents a peak at the origin of the representation. A small subset of spectra appears in the top-right corner of the distribution. We can compare this representation with those constructed using the spectral angle mapper (SAM) as shape similarity measure in figure 7. Due to the used intensity measure processing a difference between the cumulated sum of reflectance, the intensity similarity presents negative values. In this representation, the smallest distribution identified previously appears also in the top-right corner.

In order to obtain a better representation of the spectrum distribution, the reference must be chosen as sufficiently different to the spectrum to analyze. For the second experiment, we selected an equi-energetic spectrum (draw in blue in figure 5.(a)) as reference(fig. 8). As expected the BHSD shape using the KL-pseudo-divergence is fully developed without the symmetrical effect due to a reference at the center of the distribution (fig. 8.(b)). In the two BHSD using SAM and the KL-pseudo-divergence we perceive a second kernel in the main distribution, quietly sliced in shape and intensity. The smallest and isolated distribution is also preserved in the two representations as close to the equi-energetic reference. We need to be care to the negative values of intensity differences in the BHSD using the SAM measure. That explains why this representation using SAM is the symmetrical one from those using the KL-pseudo-divergence.

[4]The *Borbonicus codex* is composed of 3 sections painted between 1522 and probably 1540 with a length of 14 meters, comprising 36 fan-folded sheets each of 0.39×0.39 meter. It is stored at the *Palais Bourbon* in Paris.

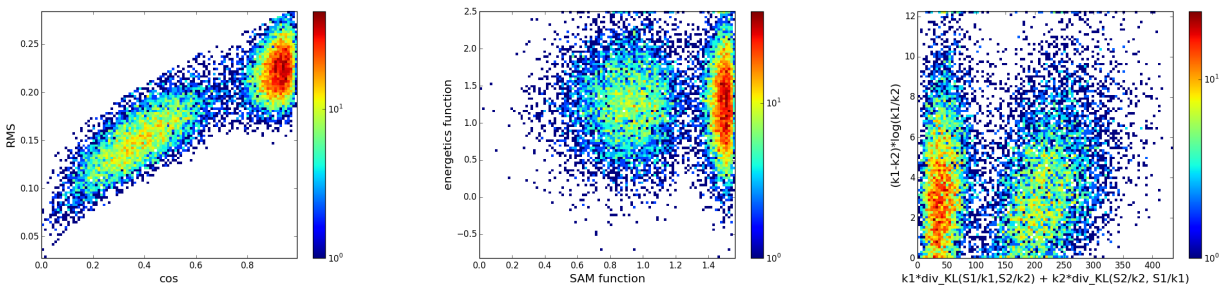

(a) NS^3 bidimensional representation (b) SAM + energy difference (c) SP-KL divergence

Fig. 3. Bidimensional Histograms of Spectral Differences (BHSD) for spectra from figure 2 using as reference the spectrum in black (fig. 2.(b)).

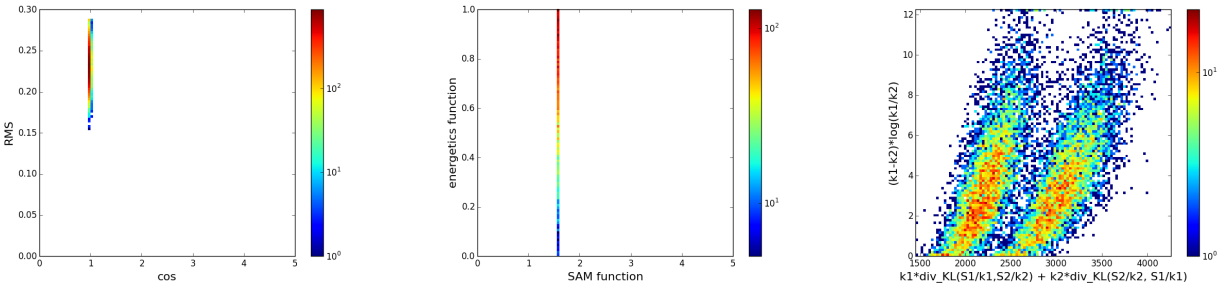

(a) NS^3 bidimensional representation (b) SAM + energy difference (c) SP-KL divergence

Fig. 4. Bidimensional Histograms of Spectral Differences (BHSD) for spectra from figure 2 using as reference the spectrum in blue (fig. 2.(b)).

Finally, we can extract some spectra corresponding to the two kernels in the main distributions[5]. The corresponding spectra are visible in figure 8.(c). As expected, we observe the small differences in intensity and shape. Such differences are difficult to identify without BHSD representations.

2) BHSD for colour contrast analysis: Working with artificial reference will be important to develop a metrology for spectral data by preserving the physical link to the optical properties of surfaces. Nevertheless, a great part of the hyperspectral imaging interest is related to the human perception of the analyzed surfaces. In this context, one of the major question is relative to the contrast assessment. In this last set of results on real data, we propose first to analyze the BHSD of the spectra corresponding to the green pixels using as reference the median spectrum corresponding to the background of the page, so the support of the painting. The average support reflectance is visible in figure 10.(c) associated to the standard-deviation of each channel. The median spectrum is the closest to the average one in the sense of the Vector Median Filter (VMF) from Astola [35]. However, the median spectrum is not blured by the averaging process. We will then observe inside a single BHSD the spectra corresponding to two different colours (red and blue) in reference to the median spectrum of the support.

In the first case, we search to observe the contrast between the green pixels and the support. In order to do that, the median spectrum from the support is extracted using the Vector Median Filter from Astola[35]. In figure 9, the two BHSD using the SAM and KL-pseudo-divergence are presented. Surprisingly, the BHSD using the SAM similarity measure is slightly modified comparing to the previous representation obtained with an equi-energetic reference. Rather than the BHSD using the KL-pseudo-divergence showing a reduced shape difference between the reference and the spectra corresponding to the green. As it can be observed in figure **??**, the difference between the equi-energetic and the support spectra is important and must induced significative differences in shape similarity. The non-linearity of the SAM similarity measure explains such results and consequently limitations. As the shape dissimilarities between the reference and the analyzed spectra are important and due to the fact that the intersection between the spectra are not null, the SAM measure looses in discrimination capacity.

[5]The spectra are extracted around the coordinates (100 ; 420) and (125 ; 580) in the BHSD using the KL-pseudo-divergence (fig. 8.(b)).

(a) Colour reproduction by CMF of page 30.

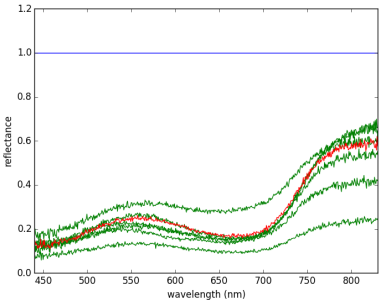

(b) Green spectra and the selected spectral references in red and blue.

(c) Corresponding colours to the selected green spectra transformed in *RGB* using CMF.

Fig. 5. Page 30 from the *Borbonicus Codex*[33] and some extracted spectra corresponding to green colour.

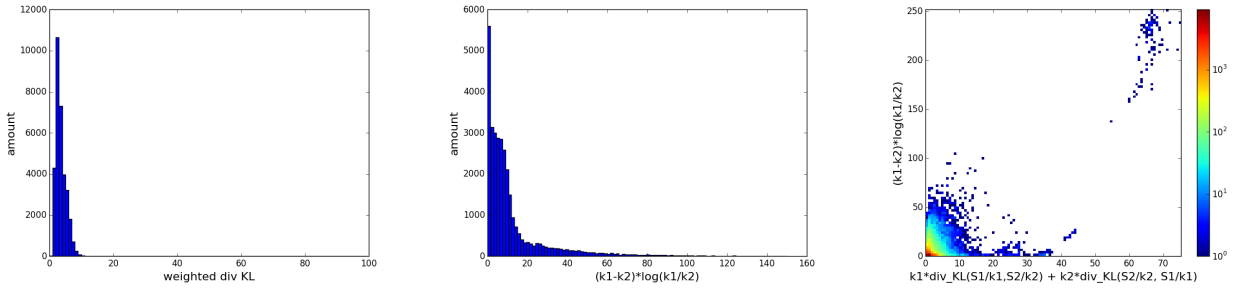

(a) Chromatic differences (b) Intensity differences (c) Bidimensional representation

Fig. 6. Unidimensional and bidimensional histograms of similarity measure from the spectral pseudo-divergence processed for the green pixels in the *codex*, distances are computed between the spectrum for each green pixel on the median green spectrum.

The second result illustrates better this lack in discrimination of the SAM measure when the shape dissimilarities are important. In this case, we construct a dataset including blue and red spectra, and we compute the BHSD using as reference the median spectrum from the support of page 30 (fig. 10). As expected, the two spectral subset are well separated in the BHSD using the KL-Pseudo-Divergence (fig. 10.(b)). The spectral distribution corresponding to the blue colour is closest from the support spectra (location : (75;90)). We observe that the intensity differences between the two colours are reduced and that the discrimination is easily performed using the shape difference part of the spectral KL-Pseudo-Divergence. By opposition this discrimination is quiet impossible when the SAM measure is used to construct the BHSD (fig. 10.(a)).

3) Discussion: These last results finish to prove the interest of the Bidimensional Histogram of Spectral Differences (BHSD) using the spectral Kullback-Leibler Pseudo-Divergence. It is possible to construct and propose other BHSD taking benefit from the existing shape similarity measures as Spectral Angle Measure (SAM), Spectral Correlation Angle Measure... But the robustness can not be ensured. Finally this result is in accordance with the remarks from Nidamanuri[15] about the limits of spectral angle measures. They are also in accordance to our previous work on the theoretical comparison of spectral distance/similarity measures[13], [14]. In these two works, it was shown that the non-linear responses of these angle measurement becomes saturated when the spectra have a null-intersection. But as previously explained such theoretical construction is never observed. Nevertheless in this work, we prove in a real case the impact of these angle measurements. The last result (fig. 10.(a)) is certainly the better illustration of these limits with the impossibility to discriminate the spectra from the blue colour from those of the red colour. Such limits are due to an unadapted definition associated to a spectrum. A spectrum can not be considered as a vector or a probability density function but as a spectral series.

Thanks to an adapted definition, we defined the spectral KL pseudo-divergence. This writing form is a valid measure, respecting the theoretical behaviour defined in [14] and respecting the decomposition proposed by Nidamanuri [15]. As demonstrated in the proposed results, the spectral discrimination is robust whatever the reference choices are. We can also note that the writing form is generic, due to relationship to the continuous integrals. Consequently, the validity proofs and bidimensional histogram representations developed in the visible domain are directly extendable to the other spectral domains.

The last element of discussion is about the spectral reference choice. The different BHSD of the green colour processed using different references are not exactly similar. These variations are expected, because each representation can be consider as a projection of the n-dimensional spectral series into a two-dimensional space defined by the reference. By changing the

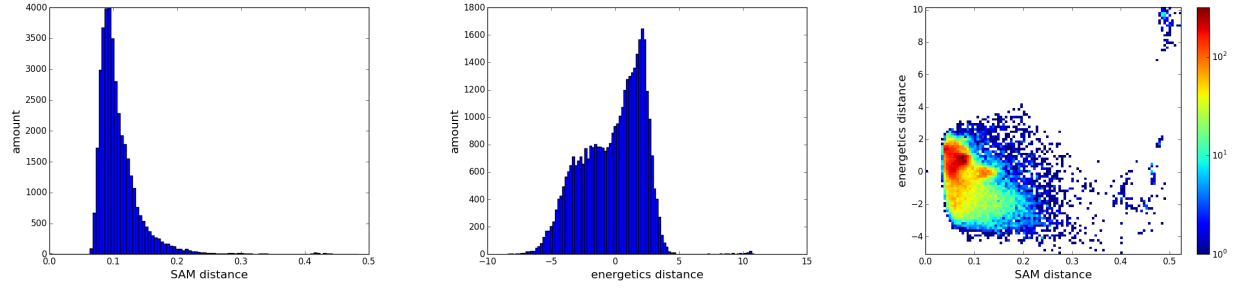

(a) Spectral Angle Mapper (b) Intensity differences (c) Bidimensional representation

Fig. 7. Unidimensional and bidimensional histograms of similarity measure from basic similarity measures for the green pixels in the *codex*, distances are computed between the spectrum for each green pixel on the median green spectrum.

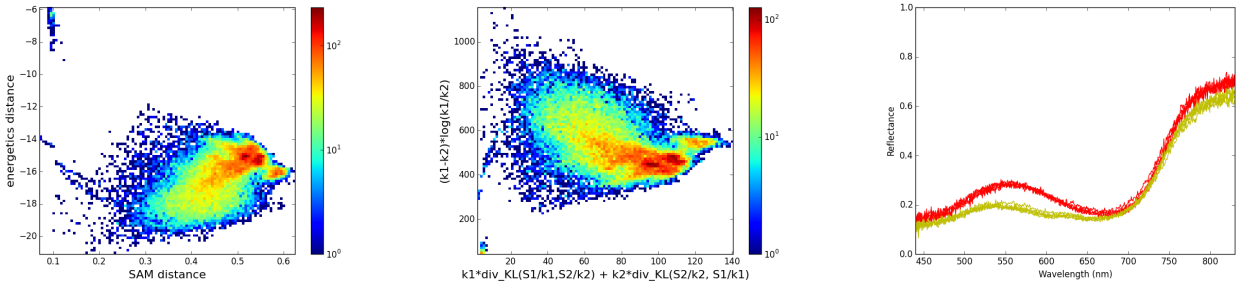

(a) SAM+Energetics. (b) KL-pseudo-divergence. (c) Extracted spectra from the main distribution and the isolated one.

Fig. 8. Bidimensional histograms of spectral differences using an equi-energetic reference and extracted spectra.

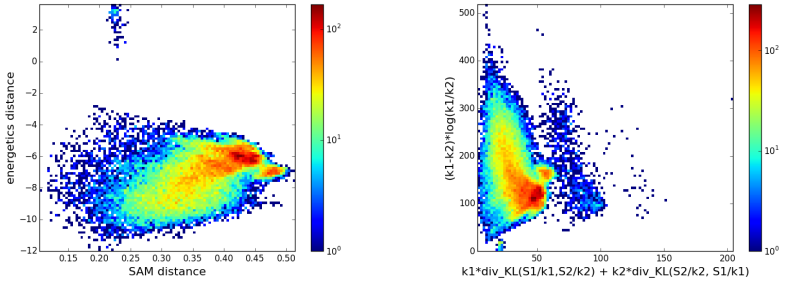

(a) SAM+Energetics. (b) KL-pseudo-divergence.

Fig. 9. Bidimensional histograms of spectral differences using as reference the median spectrum from the support.

reference, we change the point of view on these n-dimensional spectral series. So to obtain a more complete understanding about the spectral distribution, several references should be combined.

V. Conclusion

In this paper we addressed the question of the distance/similarity assessment between spectra with the objective to produce a distance/similarity function valid in accordance to the mathematical and physical sense. We selected to decompose the spectral distance/similarity measure in two parts dedicated to intensity and shape differences as proposed by Nidamanuri [15]. Measures based on Kullback-Leibler divergence are actually identified as the most efficient when applied on existing spectral image databases [16], [18], [17]. In addition in [14], it was shown that a spectrum can not be considered as a probability density function, neither as a vector. Thanks to all these bibliographic results and considering a spectrum as a spectral series, we constructed a spectral Kullback-Leibler-pseudo-divergence enabling all these constraints.

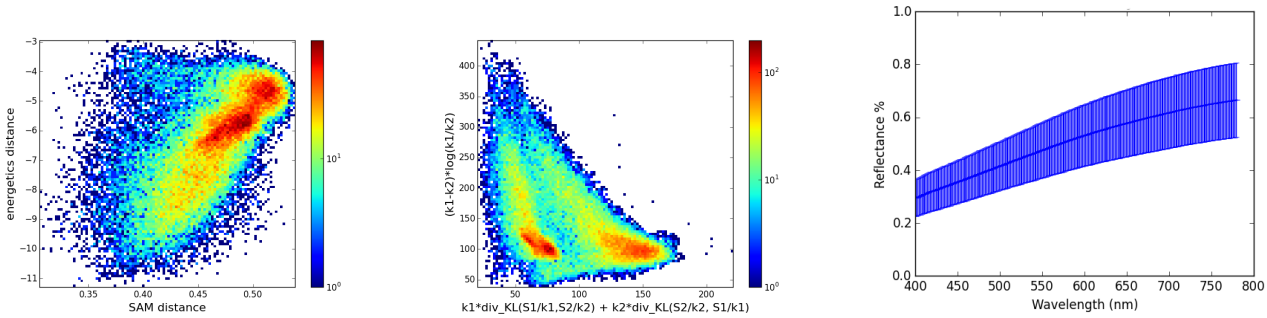

(a) SAM+Energetics. (b) KL-pseudo-divergence. (c) Mean Spectrum and standard-deviation for each spectral channel of the support reflectance.

Fig. 10. Bidimensional histograms of spectral differences of blue and red spectra using as reference the median spectrum from the support.

As a direct consequence of the similarity construction, we proposed a bidimensional representation of the spectral differences, adapted for the analysis of histograms of spectral differences. We show that such representations are easy to interpret and allow to identify the structure of the n-dimensional variations of the spectra. In the next trends, such representations will offer great perspectives in the spectrum classification.

In a real case coming from an application in Cultural Heritage, we prove the limits of others bidimensional histograms of spectral differences based on angle measurements like spectral angle mapper (SAM). In this using case, we illustrate the pigment identification problem using the proposed pseudo-divergence and the bidimensional histogram of spectral differences. The following article will assess the accuracy of the Bidimensional Histogram of Spectral Differences and the relationship to the physical content. In this following work, we will consider the combination of several references to improve the spectral discrimination between close spectra.

APPENDIX

A. Kullback-Leibler Divergence for Gaussian spectral distributions

$$h_i(x) = \frac{1}{(2\pi)^{\frac{n}{2}} |\Sigma_1|^{\frac{1}{2}}} \exp\left(-\frac{1}{2}(x-\mu_i)^t \Sigma_i^{-1}(x-\mu_i)\right), \tag{28}$$

where h_i is a density function for a multivariate Gaussian distribution with mean μ_i and covariance matrix Σ_i. $|.|$ denotes the determinant of a matrix.

Let h_1 and h_2 are two n-dimensional Gaussian spectral distributions.

Let $\tau = \mu_1 - \mu_2$ is the translation parameter and $k_1,\ k_2 \in \mathbb{R}\backslash\{0\}$.

We so have:

$$\begin{aligned} \mathrm{KL}(k_1H_1, k_2H_2) &= \frac{1}{2}\log\left(\frac{k_1}{k_2}\right) + \frac{1}{2}\log\left(\frac{|\Sigma_2|}{|\Sigma_1|}\right) \\ &\quad + \mathrm{Tr}\left(\Sigma_2^{-1}\Sigma_1\right) + \tau^t\Sigma_2^{-1}\tau - n. \end{aligned} \tag{29}$$

$$\begin{aligned} \mathrm{div}_{\mathrm{KL}}(k_1H_1, k_2H_2) &= \mathrm{Tr}\left(\Sigma_2^{-1}\Sigma_1 + \Sigma_1^{-1}\Sigma_2\right) \\ &\quad + \tau^t\left(\Sigma_1^{-1} + \Sigma_2^{-1}\right)\tau - 2n. \end{aligned} \tag{30}$$

We note that KL divergence is independant of the amplitude.

In the case of spectral distributions we so have:

$$\begin{aligned} \mathrm{KL}'(S_1, S_2) &= \frac{1}{2}\log\left(\frac{k_1}{k_2}\right) + \log\left(\frac{\sigma_2}{\sigma_1}\right) \\ &\quad + \sigma_2^{-1}\sigma_1 + \sigma_2^{-1}\tau^2 - 1. \end{aligned} \tag{31}$$

$$\mathrm{div}'_{\mathrm{KL}}(S_1, S_2) = \sigma_2^{-1}\sigma_1 + \sigma_1^{-1}\sigma_2 + \left(\sigma_1^{-1} + \sigma_2^{-1}\right)\tau^2 - 2. \tag{32}$$

REFERENCES

[1] E. Marengo, M. Manfredi, O. Zerbinati, E. Robotti, E. Mazzucco, F. Gosetti, G. Bearman, F. France, and P. Shor, "Development of a technique based on multi-spectral imaging for monitoring the conservation of cultural heritage objects," *Analytica Chimica Acta*, vol. 706, no. 2, pp. 229 – 237, 2011. [Online]. Available: http://www.sciencedirect.com/science/article/pii/S0003267011012050

[2] J. Pozo-Antonio, M. Fiorucci, A. Ramil, A. Lopez, and T. Rivas, "Evaluation of the effectiveness of laser crust removal on granites by means of hyperspectral imaging techniques," *Applied Surface Science*, vol. 347, pp. 832 – 838, 2015. [Online]. Available: http://www.sciencedirect.com/science/article/pii/S016943321501048X

[3] J. Kaufman, M. Eismann, and M. Celenk, "Assessment of spatial-spectral feature-level fusion for hyperspectral target detection," *Selected Topics in Applied Earth Observations and Remote Sensing, IEEE Journal of*, vol. 8, no. 6, pp. 2534–2544, June 2015.

[4] Working Group 2 of the Joint Committee for guides in Metrology (JCGM/WG 2), *International vocabulary of metrology - Basic and General Concepts and associated terms (VIM)*. JCGM, 2008.

[5] C. M. Cuadras, S. Valero, D. Cuadras, P. Salembierd, and J. Chanussot, "Distance-based measures of association with applications in relating hyperspectral images," *Communications in Statistics - Theory and Methods*, vol. 41, no. 13-14, pp. 2342–2355, 2012.

[6] M. Cui and S. Prasad, "Angular discriminant analysis for hyperspectral image classification," *Selected Topics in Signal Processing, IEEE Journal of*, vol. 9, no. 6, pp. 1003–1015, Sept 2015.

[7] A. Martinez-Uso, F. Pla, J. Sotoca, and P. Garcia-Sevilla, "Clustering-based hyperspectral band selection using information measures," *Geoscience and Remote Sensing, IEEE Transactions on*, vol. 45, no. 12, pp. 4158–4171, Dec 2007.

[8] A. Zare and D. Anderson, "Earth movers distance-based simultaneous comparison of hyperspectral endmembers and proportions," *Selected Topics in Applied Earth Observations and Remote Sensing, IEEE Journal of*, vol. 7, no. 6, pp. 1910–1921, June 2014.

[9] E. Zhang, X. Zhang, S. Yang, and S. Wang, "Improving hyperspectral image classification using spectral information divergence," *Geoscience and Remote Sensing Letters, IEEE*, vol. 11, no. 1, pp. 249–253, Jan 2014.

[10] S. Rousseau, D. Helbert, P. Carre, and J. Blanc-Talon, "Metric tensor for multicomponent edge detection," in *Image Processing (ICIP), 2010 17th IEEE International Conference on*, Sept 2010, pp. 1953–1956.

[11] M. Crawford, L. Ma, and W. Kim, "Exploring nonlinear manifold learning for classification of hyperspectral data," in *Optical Remote Sensing*, S. Prasad, L. M. Bruce, and J. Chanussot, Eds. Springer Berlin Heidelberg, 2011, vol. 3, pp. 207–234.

[12] D. Lunga, S. Prasad, M. Crawford, and O. Ersoy, "Manifold-learning-based feature extraction for classification of hyperspectral data: A review of advances in manifold learning," *Signal Processing Magazine, IEEE*, vol. 31, no. 1, pp. 55–66, Jan 2014.

[13] A. Ledoux, N. Richard, and A. Capelle-Laize, "How to specify or identify the most accurate multispectral distance function for non-linear image processing?" *The Colour and Visual Computing Symposium*, Sept. 2013.

[14] H. Deborah, N. Richard, and J. Y. Hardeberg, "A comprehensive evaluation on spectral distance functions and metrics for hyperspectral image processing," *Selected Topics in Applied Earth Observations and Remote Sensing, IEEE Journal of*, 2015, to appear.

[15] R. Nidamanuri and B. Zbell, "Normalized spectral similarity score ns^3 as an efficient spectral library searching method for hyperspectral image classification," *Selected Topics in Applied Earth Observations and Remote Sensing, IEEE Journal of*, vol. 4, no. 1, pp. 226–240, March 2011.

[16] S. Robila, "An analysis of spectral metrics for hyperspectral image processing," in *Geoscience and Remote Sensing Symposium, 2004. IGARSS '04. Proceedings. 2004 IEEE International*, vol. 5, Sept 2004, pp. 3233–3236 vol.5.

[17] F. Tavin, A. Roman, S. Mathieu, F. Baret, W. Liu, and P. Gouton, "Comparison of metrics for the classification of soils under variable geometrical conditions using hyperspectral data," *Geoscience and Remote Sensing Letters, IEEE*, vol. 5, no. 4, pp. 755–759, Oct 2008.

[18] F. van der Meer, "The effectiveness of spectral similarity measures for the analysis of hyperspectral imagery," *International Journal of Applied Earth Observation and Geoinformation*, vol. 8, no. 1, pp. 3 – 17, 2006. [Online]. Available: http://www.sciencedirect.com/science/article/pii/S030324340500053X

[19] J. C. Gower, "A general coefficient of similarity and some of its properties," *Biometrics*, vol. 27, no. 4, pp. 857–871, December 1971.

[20] C. C. Aggarwal, A. Hinneburg, and D. A. Keim, "On the surprising behavior of distance metrics in high dimensional spaces," in *Proceedings of the 8th International Conference on Database Theory*, ser. ICDT '01. London, UK, UK: Springer-Verlag, 2001, pp. 420–434.

[21] M.-M. Deza and E. Deza, *Dictionary of Distances*. Amsterdam, The Netherlands: Elsevier Science, 2006.

[22] F. Kruse, A. Lefkoff, J. Boardman, K. Heidebrecht, A. Shapiro, P. Barloon, and A. Goetz, "The spectral image processing system (SIPS) – interactive visualization and analysis of imaging spectrometer data," *Remote Sensing of Environment*, vol. 44, no. 2-3, pp. 145–163, 1993.

[23] J. C. Price, "How unique are spectral signatures?" *Remote Sensing of Environment*, vol. 49, no. 3, pp. 181 – 186, 1994. [Online]. Available: http://www.sciencedirect.com/science/article/pii/0034425794900132

[24] C. Rodarmel and J. Shan, "Principal component analysis for hyperspectral image classification," *Surveying and Land Information Systems*, vol. 62, no. 2, pp. 115–122, 2002.

[25] O. de Carvalho Jr., R. Guimaraes, R. Gomes, A. de Carvalho, N. da Silva, and E. Martins, "Spectral multiple correlation mapper," in *Geoscience and Remote Sensing Symposium. IEEE International Conference on*, 2006, pp. 2773–2776.

[26] O. A. Carvalho Junior and P. R. Meneses, "Spectral correlation mapper (scm): An improvement on the spectral angle mapper (sam)," in *Proceedings of Annual JPL Airborne Earth Science Workshop*, vol. 00-18. Pasadena, CA (USA): JPL-Publication, February 2000, pp. 65–74.

[27] O. A. Carvalho Junior, R. F. Guimaraes, A. R. Gillespie, N. C. Silva, and R. A. T. Gomes, "A new approach to change vector analysis using distance and similarity measures," *Remote Sensing*, vol. 3, no. 11, p. 2473, 2011. [Online]. Available: http://www.mdpi.com/2072-4292/3/11/2473

[28] F. Van der Meer and W. Bakker, "Ccsm: Cross correlogram spectral matching," *International Journal of Remote Sensing*, vol. 18, no. 5, pp. 1197–1201, 1997.

[29] D. Alman, R. Berns, T. Chong, and al., "Industrial colour-difference evaluation," CIE-Div 1-29, International Commission on Evaluation, Technical report CIE116-1995, 1995.

[30] H. Jeffreys, "An invariant form for the prior probability in estimation problems," *Royal Society of London Proceedings Series A*, vol. 186, pp. 453–461, Sept. 1946.

[31] S. Kullback and R. Leibler, "On information and sufficiency," *Annals of Mathematical Statistics*, vol. 22, no. 1, pp. 79–86, 1951.

[32] G. Mercier and M. Lennon, "On the characterization of hyperspectral texture," in *Geoscience and Remote Sensing Symposium, 2002. IGARSS '02. 2002 IEEE International*, vol. 5, 2002, pp. 2584–2586 vol.5.

[33] J. J. Batalla Rosado, "Los tlacuiloque del códice borbónico: una aproximación a su número y estilo," *Journal de la Societe des Americanistes*, vol. 80, no. 1, pp. 47–72, 1994.

[34] J. Chanda and al., "Colorimetry," CIE-TC 1-48, International Commission on Evaluation, Technical report CIE 15:2004, 2004.

[35] J. Astola, P. Haavisto, and Y. Neuvo, "Vector median filters," *Proceedings of the IEEE*, vol. 78, no. 4, pp. 678–689, April 1990.